Electronic Supplementary Material (ESI) for Journal of Materials Chemistry C.

Understanding the emission from dendrimers composed of thermally activated delayed fluorescence-based dendrons and a phosphorescent *fac*-tris[2-(thiophen-2-yl)quinoline]iridium(III) core.

Supporting Information

Junhyuk Jang,† Chandana Sampath Kumara Ranasinghe, † Akash Thamarappalli, † Mile Gao, Manikandan Koodalingam, Paul L. Burn, Emma V. Puttock, Paul E. Shaw.*

Centre for Organic Photonics & Electronics (COPE), School of Chemistry & Molecular Biosciences, The University of Queensland, St. Lucia, QLD, 4072, Australia.

† *These authors contributed equally to the work*

*p.burn2@uq.edu.au

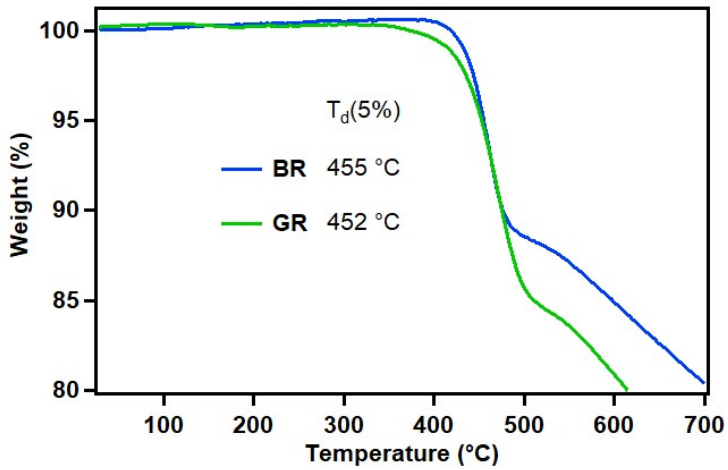

Fig. S1 TGA thermograms of **BR** and **GR** from 30-700 °C at a heating rate of 10 °C/min.

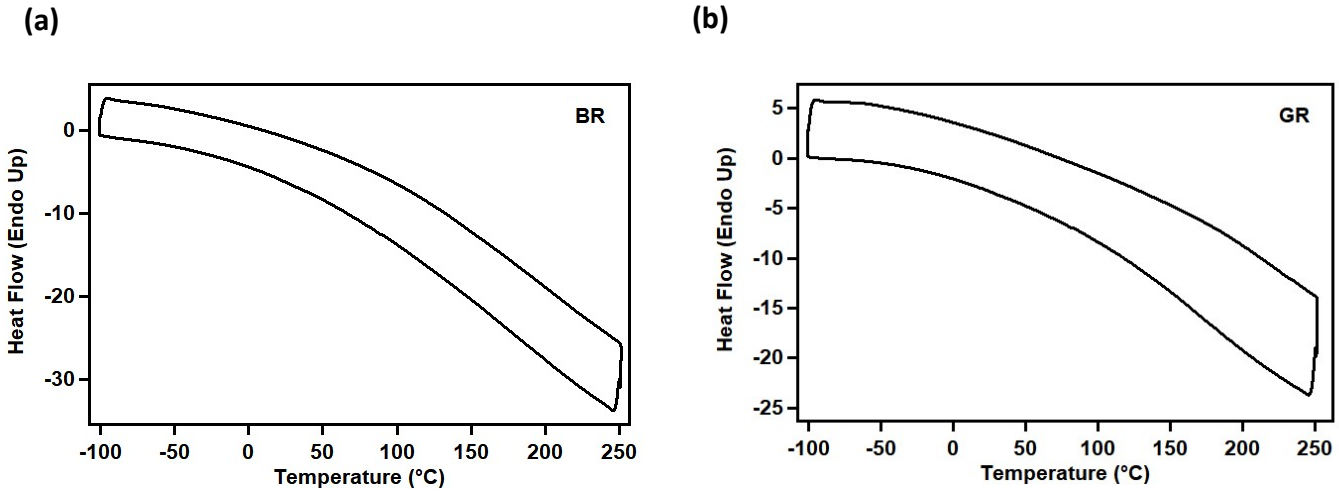

Fig. S2 DSC analysis of (a) **BR** and (b) **GR**. The measurements were performed in the temperature range of -100-250 °C at a scan rate of 50 °C/min. The second scans are shown.

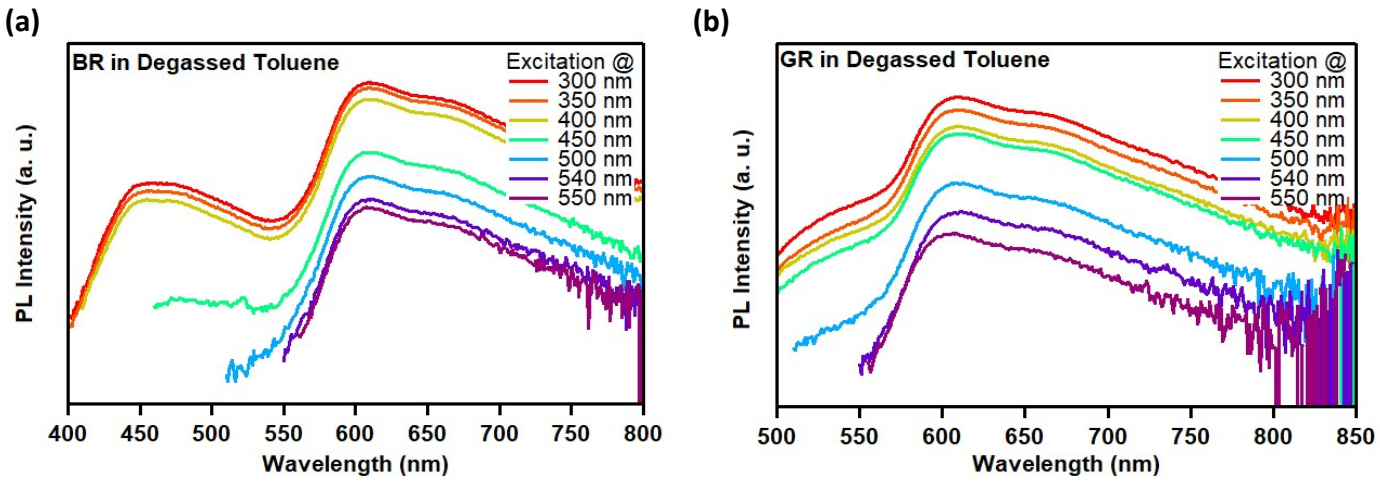

Fig. S3 PL spectra of (a) **BR** and (b) **GR** in degassed toluene measured using different excitation wavelengths.

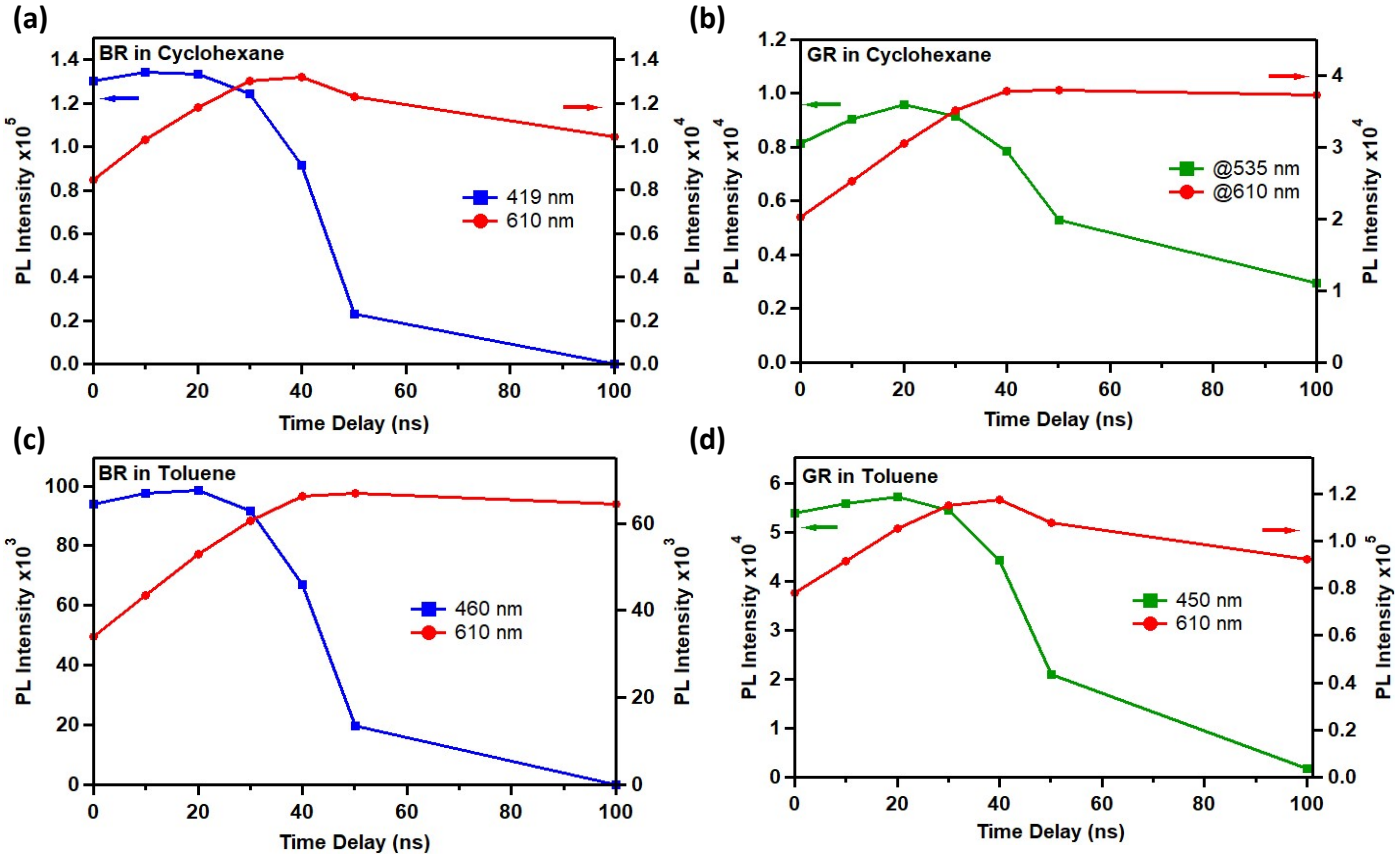

Fig. S4 Comparison of the PL intensity of the dendron and core for **BR** (left side) and **GR** (right side) in degassed cyclohexane or toluene. Excitation wavelength = 355 nm.

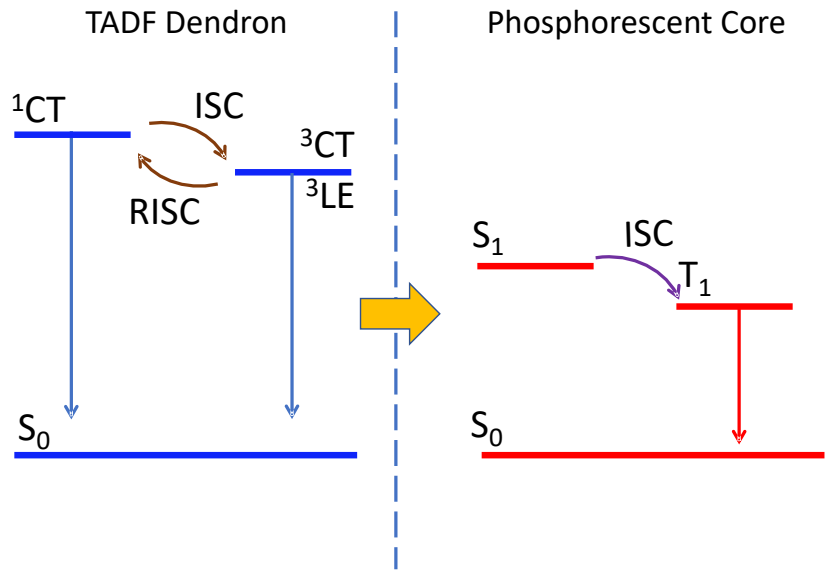

Fig. S5 Different energetic processes that can occur in the dendrimers and a pathway by which energy can be transferred from the dendrons to the emissive phosphorescent core. These include energy exchange between the TADF dendron and phosphorescent core (orange arrow) and emission processes (downwards arrows). CT = charge transfer state, LE = locally excited state, ISC = intersystem crossing, and RISC = reverse intersystem crossing.

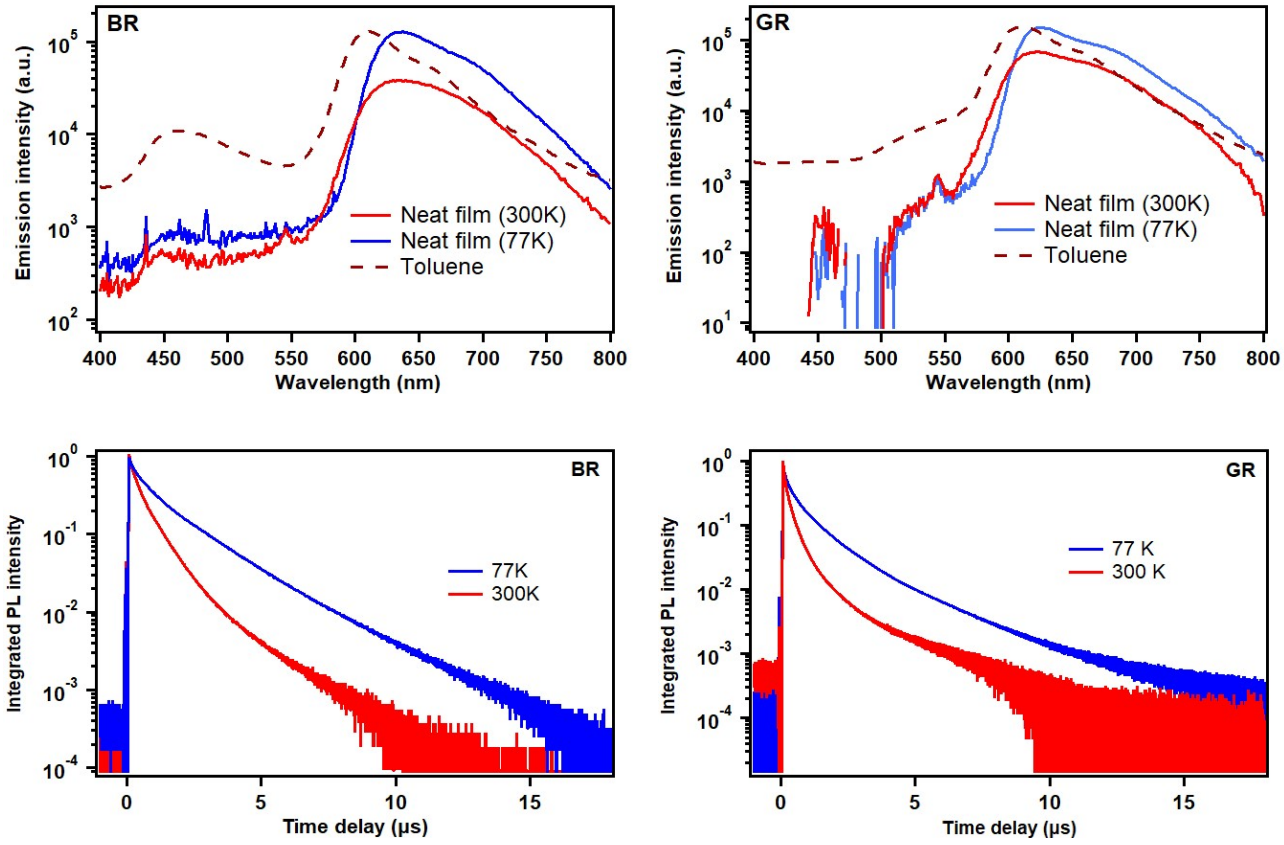

Fig. S6 Steady-state PL spectra (top) (solution and neat film) and PL decay (neat film) (bottom) of **BR** (left) and **GR** (right) at 77 K or 300 K (λ_{exc} = 355 nm).

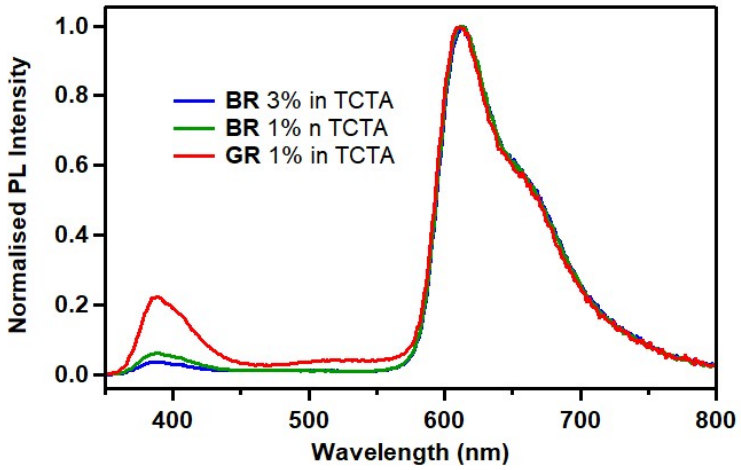

Fig. S7 Steady-state PL spectra of a solution-processed thin film of **BR** and **GR** in TCTA host.

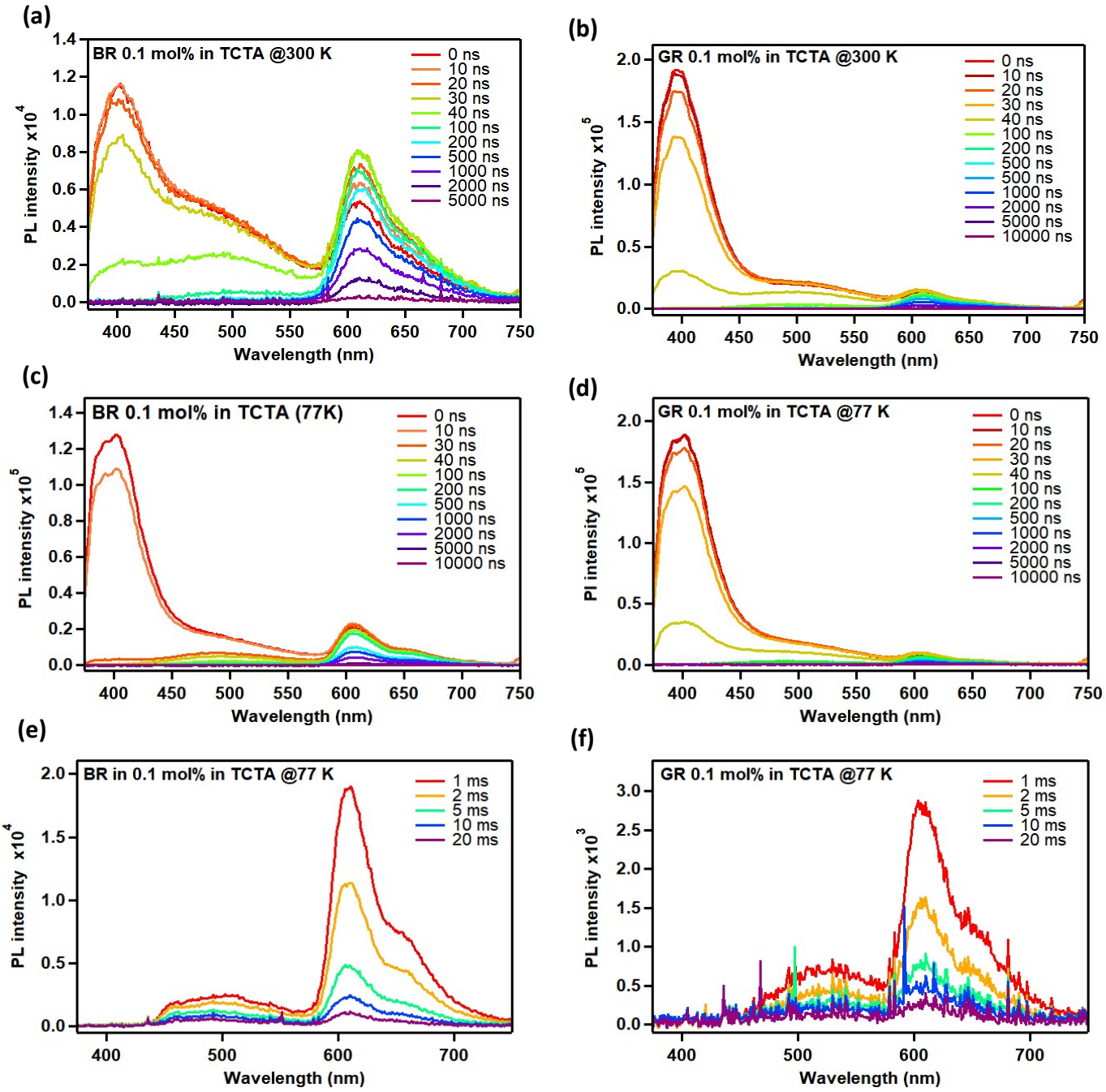

Fig. S8 Temperature-dependent spectra of a solution-processed thin film of **BR (**left) and **GR** (right) 0.1 mol% in TCTA measured at (a, b) 300 K, (c, d) 77 K, (e, f) the spectra measured at 77 K at longer times.

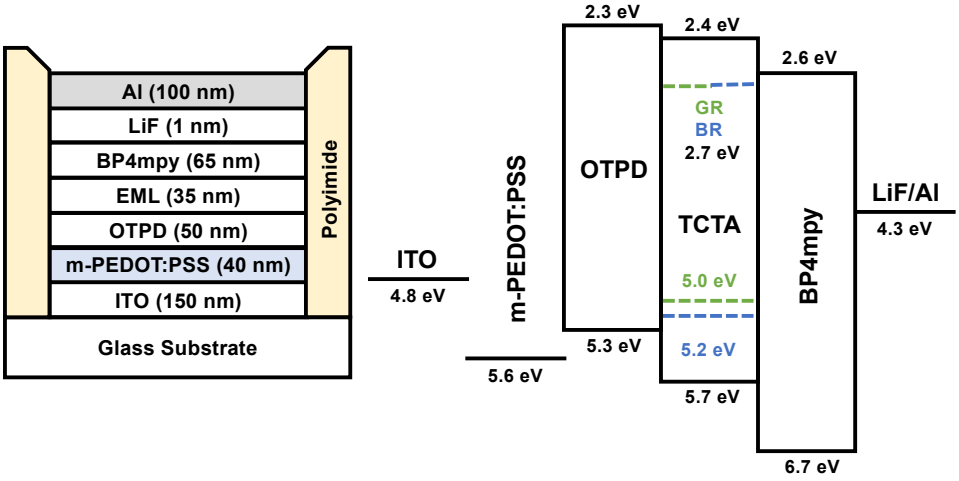

Fig. S9 Schematic device architecture and the energy levels. The energy levels are taken from the literature apart from the dendrimers, which are calculated from their first oxidation and reduction potentials and referenced against the ionisation potential of ferrocene (4.8 eV).

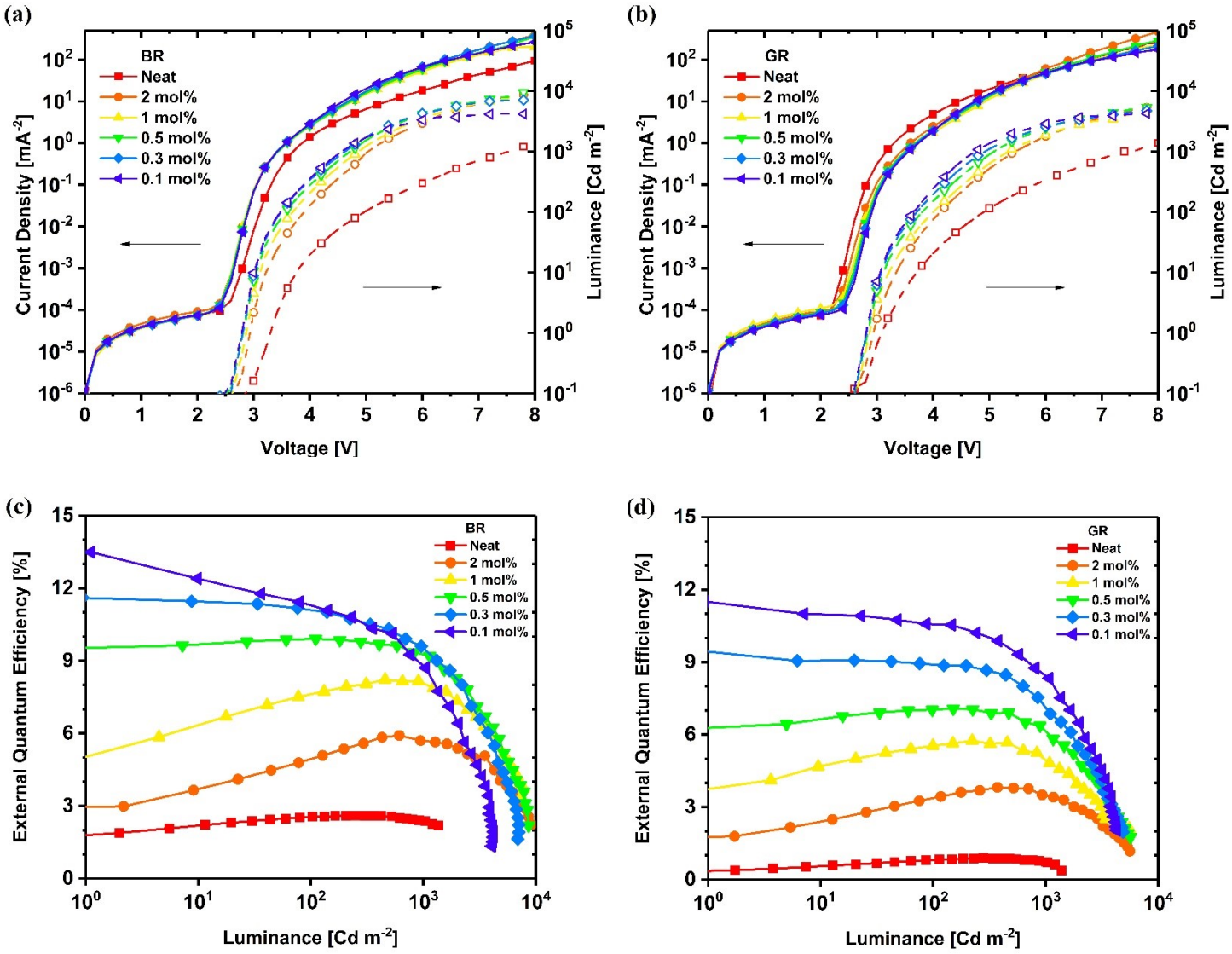

Fig. S10 (a) and (b) Current Density-Voltage-Luminance characteristics of **BR** and **GR** at different concentrations, (c) and (d) External Quantum Efficiency (EQE)-Luminance characteristics of **BR** and **GR** in different blending ratios.

Table S1 Device performance characteristics of the OLEDs composed of **BR** and **GR** contaning films of different blending ratio.

BR ratio [mol %]	Turn-on Voltage [V]	Max. EQE [%]	Max. Luminance [Cd m^{-2}]	GR ratio [mol %]	Turn-on Voltage [V]	Max. EQE [%]	Max. Luminance [Cd m^{-2}]
Neat	3.3	2.6	1,373	Neat	3.1	0.9	1,387
2	2.9	5.9	9,158	2	2.9	3.8	5,607
1	2.9	8.2	8,639	1	2.9	5.7	5,532
0.5	2.8	9.9	7,799	0.5	2.8	7.1	5,669
0.3	2.8	11.5	6,905	0.3	2.8	9.1	4,885
0.1	2.8	13.5	4,216	0.1	2.8	11.0	4,272

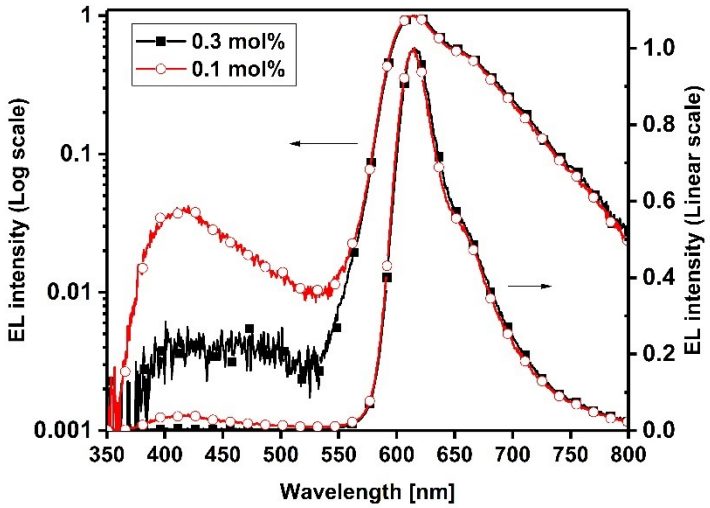

Fig. S11 Electroluminescence spectra of OLEDs with 0.1 mol% or 0.3 mol% of **BR** in the EML at 8.0 V.

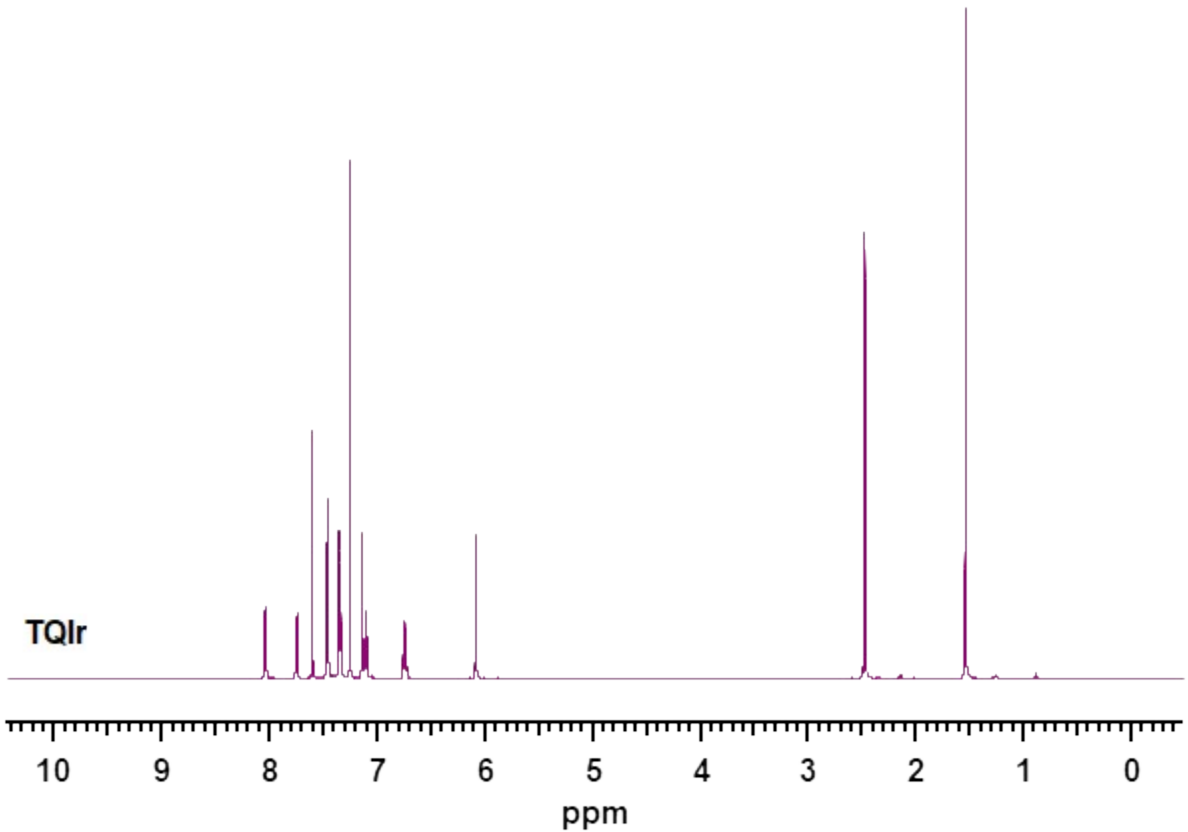

Fig S12 [1]H NMR spectrum of **TQIr** measured in deuterated chloroform.

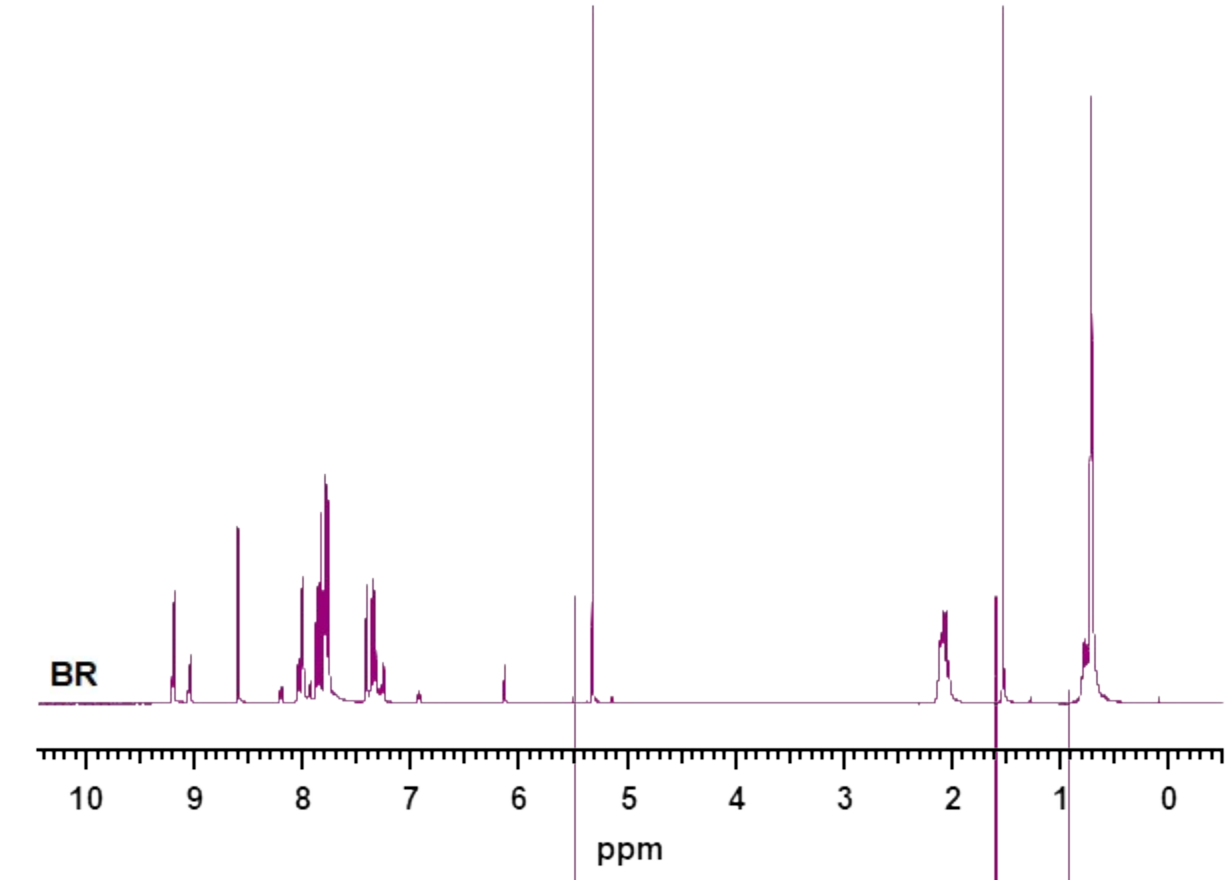

Fig S13. [1]H NMR spectrum of **BR** measured in deuterated dichloromethane.

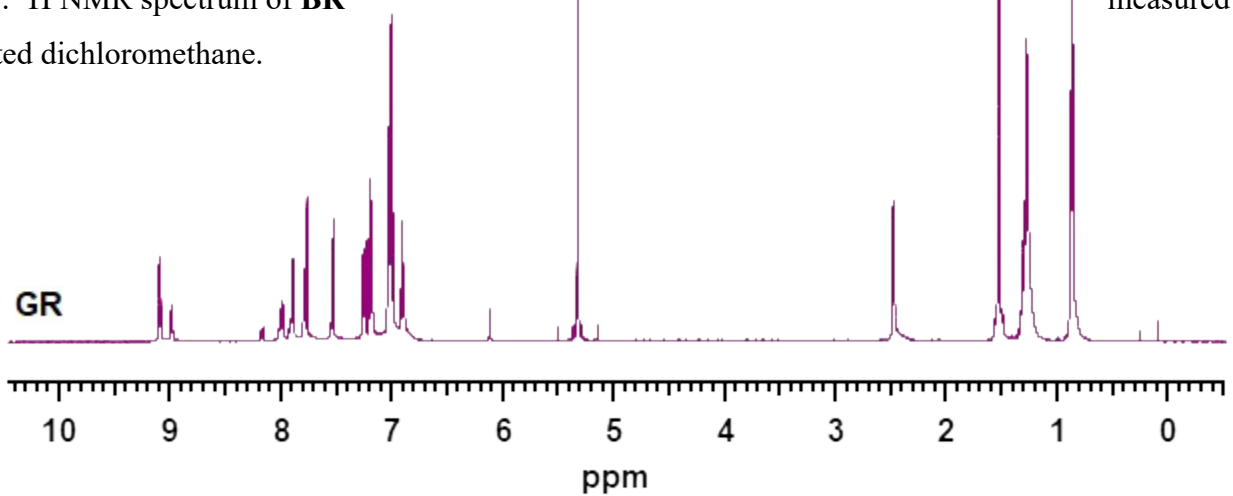

Fig. S14 ^{1}H NMR spectrum of **GR** measured in deuterated dichloromethane.